Escherichia coli inactivation by N, S co-doped commercial TiO$_2$ powders under UV and visible light

J.A. Rengifo-Herrera [a], E. Mielczarski [c], J. Mielczarski [c], N.C. Castillo [a], J. Kiwi [b], C. Pulgarin [a,*]

[a] Institute of Chemical Sciences and Engineering, SB, GGEC Station 6, Ecole Polytechnique Fédérale de Lausanne, 1015 Lausanne, Switzerland
[b] Institute of Chemical Sciences and Engineering, SB, LGRC, Station 6, Ecole Polytechnique Fédérale de Lausanne, 1015 Lausanne, Switzerland
[c] INPL/CNRS, UMR 7569 LEM, 15 Av de Charmois, 54501 Vandoeuvre les Nancy, France

ARTICLE INFO

ABSTRACT

Commercial anatase TiO$_2$ powders (Tayca TKP101, TKP102) were ground with thiourea and annealed at 400 and 500 °C. Diffuse reflectance spectra (DRS) showed that the doping with thiourea shifted the TiO$_2$ absorption towards the visible region. The absorption was observed to increase with increasing annealing temperature. Using the Kubelka–Munk relations, it was possible to determine the band-gap of the doped TiO$_2$. Doped Tayca TiO$_2$ TKP101 showed a band-gap of 2.12 and 2.24 eV calcined at 400 and 500 °C, respectively. Doped Tayca TiO$_2$ TKP102 calcined at 400 and 500 °C showed in both cases a band-gap of 2.85 eV. X-ray photoelectron spectroscopy (XPS) revealed that these doped TiO$_2$, TKP101 annealed at 400 °C and TKP102 annealed at 400 and 500 °C present interstitial N-doping while doped TKP101 annealed at 500 °C showed a peak characteristic of substitutional N-doping. S-doped materials calcined at 500 °C presented only anionic S-doping. Nitrogen adsorption studies (BET) showed a loss of specific surface area (SSA) in annealed TiO$_2$ samples. N- and S co-doped materials showed suitable photocatalytic activity under UV illumination towards Escherichia coli inactivation and also under visible light irradiation (400–500 nm). Applying different annealing temperatures led to a variety of structures for N and S incorporated in the crystalline network. TiO$_2$ upon annealing showed a varying degree of hydroxylation and particles sizes. This seems to affect the trapping and transfer of the charge carriers generated under light and the semiconductor performance.

© 2008 Elsevier B.V. All rights reserved.

1. Introduction

The development of photocatalytic processes to inactivate pathogenic agents in aqueous media is a matter of growing interest. Indeed, conventional drinking water disinfection procedures, such as chlorination and ozonization, can generate disinfection by-products (DBPs) with carcinogenic and mutagenic potential [1]. Solar disinfection processes are of particular interest for this kind of treatment in areas having intense solar exposure. Solar irradiation can activate photocatalysts such as TiO$_2$, ZnO or WO$_3$ due to their UV-component generating electron–hole pairs and leading to hydroxyl (•OH) and superoxide (•O$_2^-$) radicals [2–6], both considered as reactive oxygen species (ROS) having biocidal activity against waterborne bacteria [7–11].

TiO$_2$ is one non-toxic and stable photocatalyst. However, it absorbs only about 4% of the solar irradiation. The absorption broadening of TiO$_2$ towards the visible region could be favorable for its performance in drinking water disinfection. TiO$_2$ catalysts with visible light response have been already reported by anchoring of organic or inorganic dyes on the surface of TiO$_2$ [12–14], doping by metal ions [15–18] and by introducing oxygen vacancies that generate color centers reducing the band-gap of TiO$_2$ (3.1–3.2 eV) [19–21].

More recently, another approach has been developed to dope TiO$_2$ with non-metallic species such as N, S and C leading to a spectral shift towards the visible region. Nitrogen, carbon and sulfur doping of TiO$_2$ have been carried out for sol–gel TiO$_2$ [22–24] from TiCl$_4$ or titanium tetra-isopropoxide (TTIP) using N-, S- and C-precursors. The doping of commercial TiO$_2$ powders has also been explored [25–27]. It has been claimed that the oxygen vacancies generated during the doping are responsible for the visible light absorption [28]. Band structure calculations of N-doped TiO$_2$ led Asahi et al. [29] to suggest that oxygen sites were substituted by N atoms leading to the shift of the valence band by the mixing of the 2p orbital of both elements. This in turn led to the narrowing of the

TiO_2 band-gap. More recently Livraghi et al. [30] and Di Valentin et al. suggested that N-doping favors oxygen vacancies formation [31,32]. C-doped TiO_2 [33] and S-doped TiO_2 have also been recently reported [34].

The photoactivity of C-, N- and S-doped TiO_2 in reactions leading to the degradation of pollutants [23,24,35,36] has been reported to be higher than to the non-doped TiO_2 under visible light irradiation. Also some studies on the bacterial inactivation with N-, C- and S-doped TiO_2 have been reported [37–40]. Two studies have reported the detailed preparation of N, S co-doped TiO_2 powders [41,42]. We present hereby the photocatalytic activities of co-doped anatase powders tested to inactivate *Escherichia coli* cells under two different light sources: UV light (330–400 nm) and blue light (400–500 nm). We also present the first evidence for photocatalytic bacterial inactivation with N, S co-doped commercial powders. In this study we report a simple method to prepare commercial anatase TiO_2 powders co-doped by N and S by the use of thiourea as doping source. Tayca TKP powders were selected since in a previous report out of our laboratory, the powder Tayca TKP101 showed a similar photocatalytic activity towards *E. coli* inactivation than Degussa P-25 powders [11] and in our work for the first time Tayca TKP102 is tested to inactivate *E. coli*.

2. Experimental

2.1. Materials

Two commercial types of photocatalytic TiO2 powders: Tayca TKP101 (anatase form and purity of 86%) and Tayca TKP102 (anatase form and purity of 96%) were used as obtained from Tayca Corporation. Bidistilled Milli-Q water was used throughout this study. Thiourea was purchased from Sigma Aldrich (99%).

2.2. Powders preparation

Doped TiO_2 was prepared by mechanical mixing of thiourea with TiO_2 in a 4:1 ratio. The materials were annealed under air atmosphere during 1 h either at 400 or 500 °C with a heating rate of 10 °C for minute and cooled at room temperature. After heating the materials were washed with Milli-Q water three times and dry at 70 °C and then crushed in an agate mortar into a fine powder before use.

2.3. Powders characterization

2.3.1. Diffuse reflectance UV–vis spectroscopy

Diffuse reflectance spectra (DRS) of TiO_2 powders were measured with a Varian Casy 1E spectrophotometer equipped with a diffuse reflectance accessory. The Kubelka–Munk relations [43] were used to transform the reflectance data into absorption spectra. A Kodak analytical standard white reflectance coating was used as reference. Diffuse reflectance can be related to the absorbance by the K/S ratio using the Kubelka–Munk relations ($F(R_\infty)$) (Eq. (1)), where the scattering is noted as S and reflectance is noted as R. The reflectance relates to the absorption coefficient α (K/S) and this is proportional to absorbance K (Eq. (1)).

$$\frac{K}{S} = \frac{(1 - R_\infty)^2}{2R_\infty} \equiv F(R_\infty) \tag{1}$$

2.3.2. X-ray photoelectron spectroscopy (XPS)

XPS analyses were carried out on a XPS Analyzer Kratos model Axis Ultra with a monochromatic AlKα and charge neutralizer.

The deconvolution software program was provided by Kratos the manufacturer of the XPS instrument. This program is the standard program used by a large number of people working in the field and is accepted as reference in the field.

All the binding energies were referenced to the C 1s peak at 285 eV of carbon. Powder samples were prepared by deposition of catalyst on carbon type stuck to sample holder. The powder samples were analyzed with very large spot with dimension 0.3 mm × 0.7 mm. Therefore, it is assumed that the recorded spectrum is characteristic for "average" particles. Using a large spot we improved significantly the signal/noise ratio.

The atomic concentrations were determined with an increased sensitivity factor because in general the signal/noise ratio is weak. This analysis was carried out: (a) taking a larger area. (b) The signal accumulation time was increased and (c) the elements analyzed like N did not have a weak sensitivity. The detection limit was not 0.1 at.% but 0.03 at.%.

2.3.3. Specific surface area (SSA)

Specific surface areas (SSAs) were measured using nitrogen adsorption–desorption at 77 K via a Sorptomatic 1990 instrument (Carlo Erba) and calculated using the BET method.

2.3.4. Photocatalytic activity

Cylindrical Pyrex bottles (50 mL) were used, a TiO_2 concentration of 1.0 g L^{-1} was selected and oxygen (present in the air) was used as electron acceptor. The suspension was kept under magnetic stirring and it was irradiated by five Black light lamps Phillips TLD 18W (emission spectra: 330–400 nm and UV intensity between 300 and 400 nm: 38 W m^{-2}) and five fluorescent lamps Phillips TLD-18W blue (emission spectra: 400–500 nm. UV intensity: 0.1 W m^{-2} and intensity between 290 and 1100 nm: 60 W m^{-2}). The radiant flux was monitored with a Kipp & Zonen (CM3) power meter (Omni instruments Ltd., Dundee, UK). Temperature of the experiments was never superior to 38 °C. Samples were periodically collected to follow the reaction kinetics. Results represent the average of three experimental runs and their standard deviations were equal or lower than 15%.

2.3.5. Bacterial inactivation

Photocatalytic activity in bacterial inactivation was measured by sampling from the photoreactor an *E. coli* strain K12 MG 1655. Before the experiment, bacteria were inoculated into nutrient broth (Oxoid no. 2, Switzerland) and grown overnight at 37 °C. During the stationary growth phase, bacteria cells were harvested by centrifugation at 5000 rpm for 10 min at 4 °C. The bacterial pellet was then washed three times with a saline solution (8 g L^{-1} NaCl and 0.8 g L^{-1} KCl in Milli-Q water, pH 7 by addition of HCl or NaOH). A suitable cell concentration (10^4 CFU mL^{-1}) was inoculated in the reactor's saline solution. Then, the inoculated Pyrex bottles with the catalyst added were illuminated during 2 h and samples (1.0 mL) were taken at different time intervals. Serial dilutions were performed in saline solution and 100 µL volumes were inoculated in a plate count agar (PCA, Merck, Germany) growth medium. The number of colonies was counted 24 h after inoculation at 37 °C. Control experiments (*E. coli* and UV or visible light without catalyst) and (*E. coli* + catalyst without light) were also performed.

3. Results and discussion

3.1. Doped TiO₂ powders characterization

3.1.1. Diffuse reflection spectroscopy and Kubelka–Munk relations

Fig. 1a and b shows the K/S ratio variation vs. the applied wavelength. The non-doped powder TKP101 (Fig. 1a) starts to
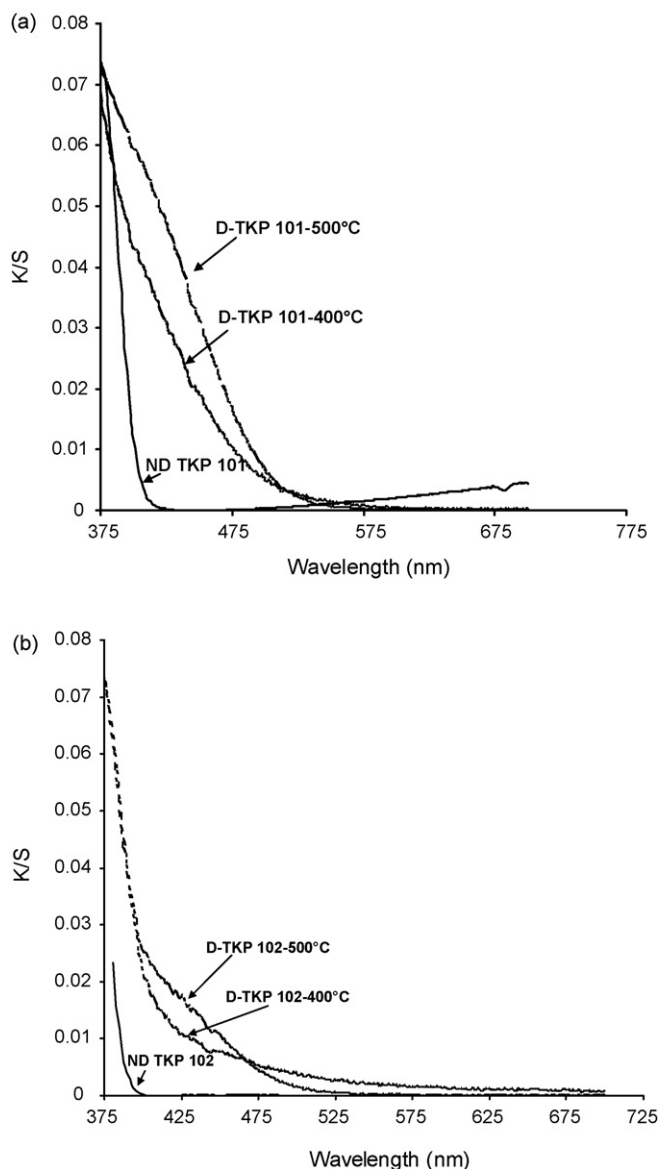
(a)

(b)

Fig. 1. UV–vis spectra of TiO$_2$ powders. (a) TKP101 and (b) TKP102.

Table 1
Band-gap estimation for non-doped and doped commercial TiO$_2$

Powder	Estimated E_{bg} (eV)
Undoped Tayca TKP101	3.02
N, S Tayca TKP101-400 °C	2.12
N, S Tayca TKP101-500 °C	2.24
Undoped Tayca TKP102	3.21
N, S Tayca TKP102-400 °C	2.85
N, S Tayca TKP102-500 °C	2.85

respectively, but TKP102 powders presented a band-gap narrowing of 0.36 eV.

3.1.2. X-ray photo-spectrometry measurements (XPS)

XPS measurements were made to determine the species responsible for the light absorption widening. We focused on the N 1s, S 2p, and O 1s peaks, since we did not observe any modification in the Ti peaks. Adventitious C 1s peaks were observed due to contamination during the synthesis of the TiO$_2$ and the presence of carbonates. Both carbonaceous species are not responsible of TiO$_2$ visible response.

Fig. 2a–c shows N 1s peak of pure and thiourea doped Tayca TKP101 powders. TKP101 pure TiO$_2$ peaks present binding energies (BEs) of 400 and 402 eV. These peaks have been related to N-species adsorbed on the TiO$_2$ surface such as NO, NO$_2$ or N$_2$ [44–48].

Today a controversy exists about the assignation of XPS N 1s peaks in N-doped TiO$_2$ powders. N 1s peaks has been found at BE of 396, 398, and BE > 400 eV. Peaks localized at 396 and 398 eV have been assigned to anionic N-doping (substitution of O by N) [29,44,46,49,50]. On the other hand, some authors have assigned the peaks at BE > 400 eV to interstitial N-doping (addition of N atom to the O atoms on the TiO$_2$ surfaces). In this work, doped TKP101 powders annealed at 400 °C showed N 1s peaks at 399.7 and 402 eV, in agreement with the values reported by Yates of 399.6 eV [51]. The peak at 402 eV has been reported by Gopinath et al. as due to NO or NO$_2$ species [52]. Both authors, suggested that N 1s peaks with BE at 399.6 and BE > 400 eV are due to interstitial N–TiO$_2$ and/or the formation of O–N–Ti species.

The N 1s peak in doped TKP101 powders calcined at 500 °C showed three peaks by deconvolution at 395.9, 398.4 and 400.5 eV. The peak at 395.9 eV is assigned to anionic N-doping where O is replaced by N atoms involving substitutional N-doping [29,44,46,49,50] and the peak at 398.4 eV is also due to anionic N-doping but incorporated in the TiO$_2$ as N–Ti–O structural feature [52]. Finally, the peak at 400.5 V is attributed to O–N–Ti species [53]. Two S 2p peak were detected in pure TKP101 powder at BE > 168 eV and 165 < BE < 163 eV. Deconvolution of these peaks did not show the presence of S-doped TiO$_2$ peaks. Both peaks are probably due to presence of impurities of adsorbed sulfurous species on the TiO$_2$ surfaces (such as: SO$_4$, SO$_2$ or SO). However, when the powders were treated with thiourea at 400 and 500 °C it was possible to identify peaks involving S-doped TiO$_2$ species.

In doped powders calcined at 400 °C two peaks at 162.4 and 167.8 eV were found. Previous works have assigned the peak at 162.4 eV to substitution of O of TiO$_2$ due to S anionic doping [24,34,54–56]. If the sulfur is about the same in the undoped and the doped samples this is not the important question to address. In the doped sample four different peak positions were found for sulfur and one of them at 162.4 eV corresponding to sulfide (S^{-2} anionic sulfur) did parallel the catalytic activity of the doped sample. This is the experimental evidence for the presence of catalytic sulfide in the doped samples that is absent in the starting material. Ohno et al. [24] have suggested that the presence of the

absorb at $\lambda < 410$ nm and undoped TKP102 at $\lambda < 400$ nm. The observed absorption of pure TKP102 is typical for anatase while pure TKP101 (also anatase) absorbs at $\lambda < 410$ nm, probably due to the presence of surface defects. It is well known that surface defects produce a red shift on the TiO$_2$ absorption [19–21]. Calcination of non-doped powders did not show any alteration in their DRS spectra (data not showed).

Thiourea treated TKP101 and TKP102 powders annealed at 400 °C showed an ivory coloration while treated TKP101 powder annealed at 500 °C showed an intense yellow color. Their DRS spectra show a shoulder between 400 and 550 nm in addition to the typical absorption of anatase TiO$_2$ ($\lambda < 400$ nm). The absorption in the visible region increases with the temperature, but this increase was more marked in the case of the TKP101 powders.

The Kubelka–Munk relations were also used to determine the band-gap energies of the doped powders. Band-gap energy of pure TiO$_2$ (3.2 eV for the TiO$_2$) matched the values reported for anatase. The band-gaps of several doped TiO$_2$ prepared during this study is shown in Table 1. Band-gap narrowing of around 0.9 and 0.78 eV was observed for TKP101 powders calcined at 400 and 500 °C,

peak at 167.8 eV was probable due to substitution of Ti by S due to cationic doping. Doped TKP101 powders calcined at 500 °C did not reveal a peak at 162 eV, but it revealed a peak at 167.8 eV due to cationic S-doping of TiO_2. The XPS of pure TKP102 powders did not reveal the presence of N and S impurities. These species were only observed when the powder was treated with thiourea and calcined at 400 and 500 °C (Fig. 2d and e). Doped TKP102 calcined at 400 °C showed the formation of N 1s peaks at 399.2 and 400.7 eV. If the

calcinations temperature was raised to 500 °C, then N 1s peaks at 402.1 and 399.9 eV were observed and assigned to interstitial N-doping of TiO_2 and also the formation of O–N–Ti linkage. S 2p peaks in doped TKP102 calcined at 400 °C revealed the presence of substitutional anionic S-doping at 162.8 eV and substitutional cationic S-doping at 167.2 eV. TiO_2 TKP102 annealed at 500 °C showed an S 2p peak at 167.6 eV probably due to cationic S-substitution. The peaks at BE > 168 eV present in TKP101 and
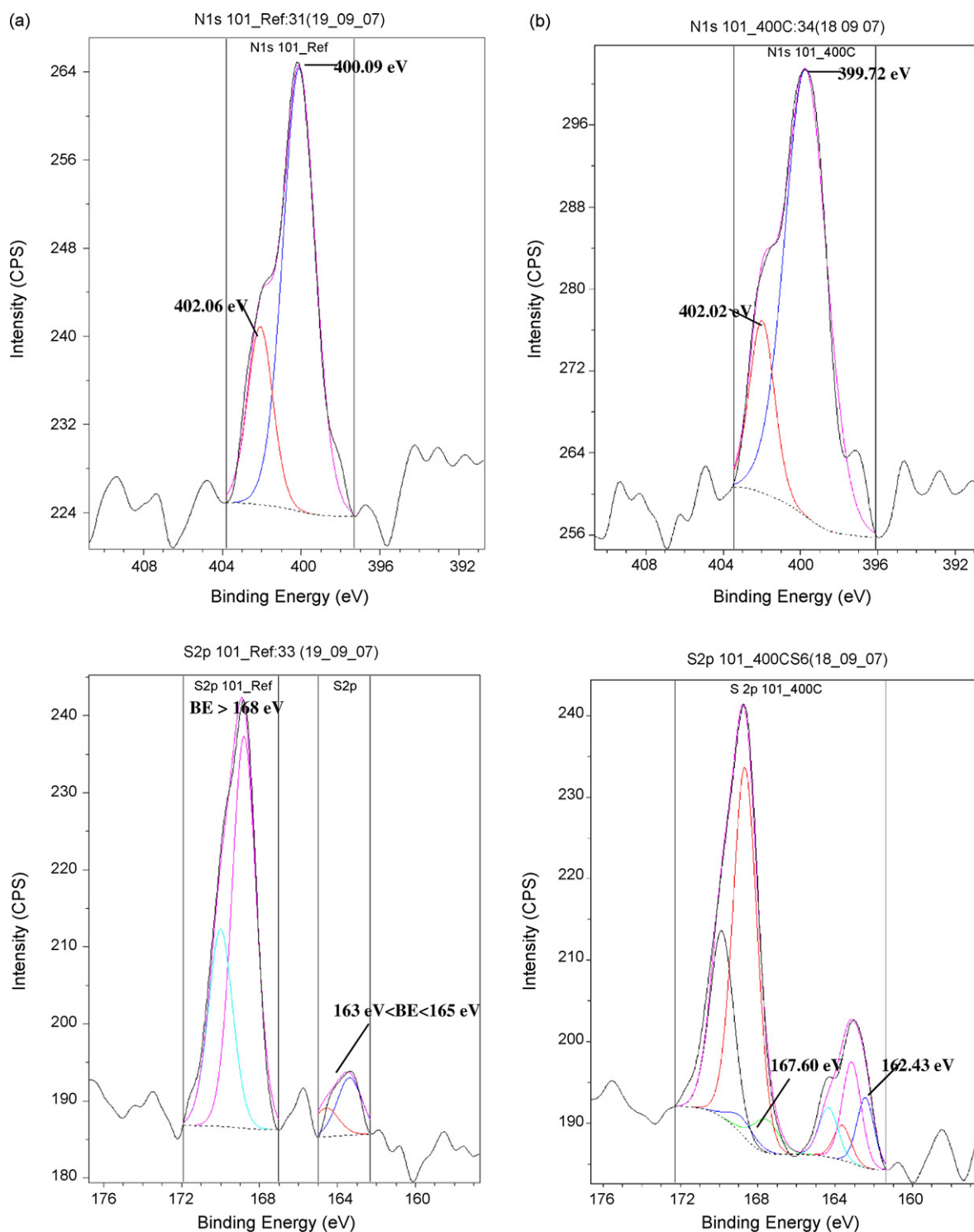

Fig. 2. (a) Deconvolution N and S XPS peaks of (a) non-doped TKP101 powder, (b) thiourea treated TKP101 powder annealed at 400 °C, (c) thiourea treated TKP101 powder annealed at 500 °C, (d) thiourea treated TKP102 powder annealed at 400 °C, and (e) thiourea treated TKP102 powder annealed at 500 °C.
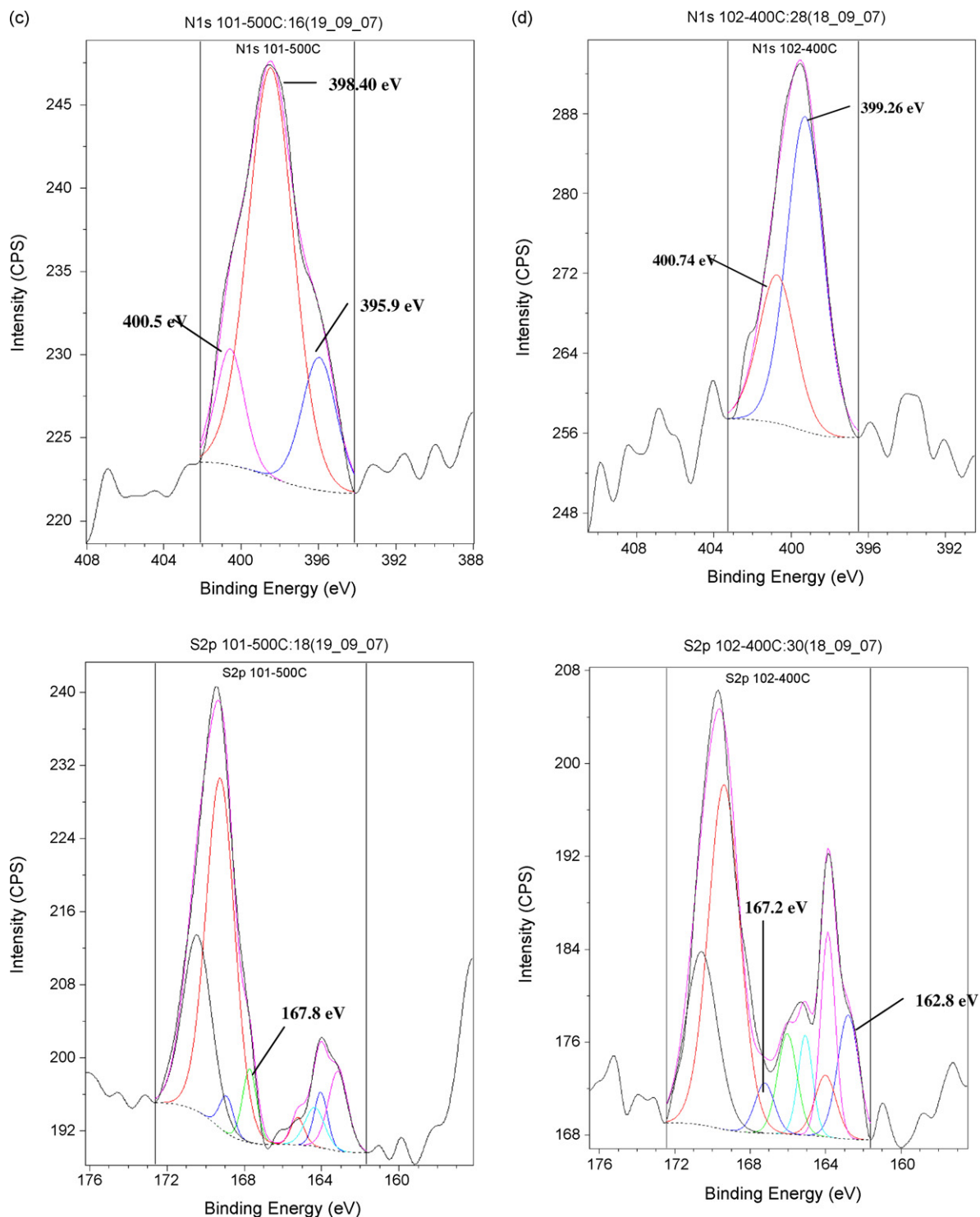
Fig. 2. (*Continued*)

TKP102 annealed at 400–500 °C can be ascribed to the formation of pyrosulfate, SO_4^{2-} and SO_2 [57] produced during the combustion of thiourea.

Regarding the O 1s in Fig. 3a and b a peak at 530 eV was found in pure TKP101 and TKP102 powders due to Ti–O link. However, a shoulder at BE > 531 eV was also found due to presence of surface hydroxyl groups, water, carbon, nitrogen and sulfur oxide. Our assignation of O 1s peak is in variance with the conclusions obtained by Gyorgy et al. [58] and Chen and Burda [59]. They

suggested that the observed shoulder was due to formation of Ti–N that by oxidation leads to Ti–O–N and O–Ti–N. However, we suggest that this peak is probably due to presence of hydroxyl groups, NO, SO, CO species or water on the surface. This would explain the decrease observed for this peak when the calcination temperature was increased.

Theoretical studies carried out by Di Valentin et al. [31] have suggested the existence of two types of N-doping: interstitial and substitutional. Both types of doping depend of the preparation
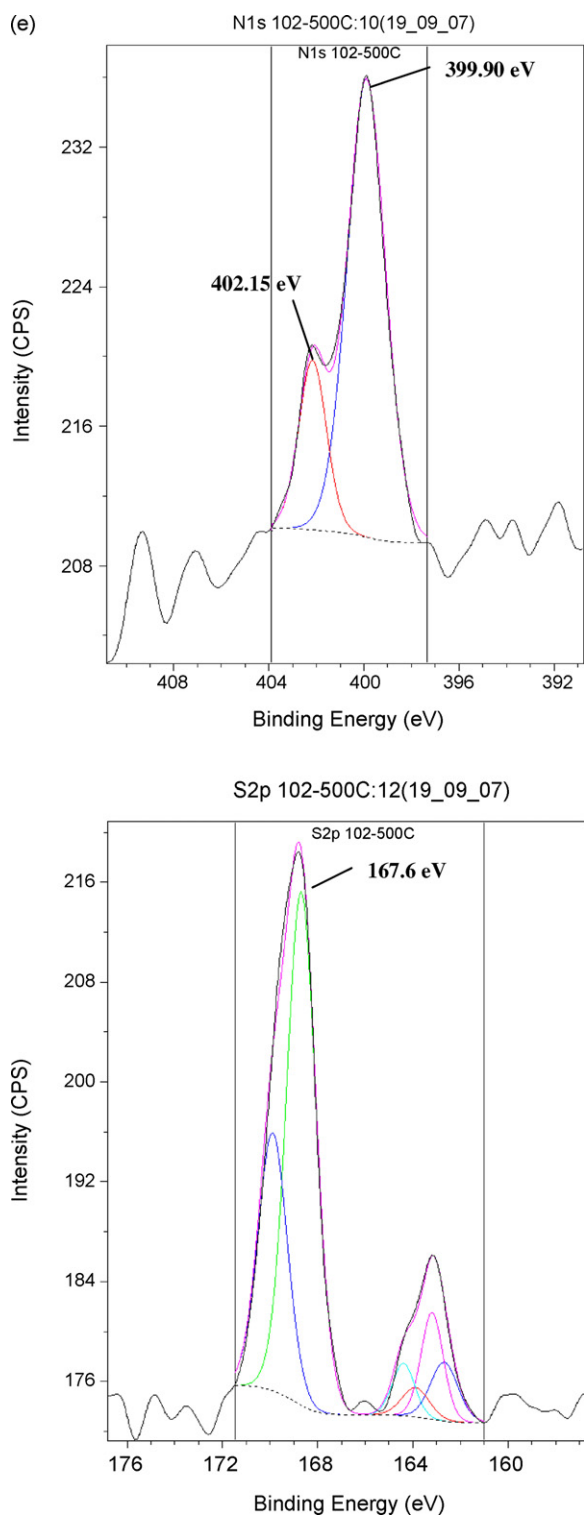
(e)

N1s 102-500C:10(19_09_07)

N1s 102-500C

399.90 eV

402.15 eV

S2p 102-500C:12(19_09_07)

S2p 102-500C

167.6 eV

Fig. 2. (*Continued*).

01s 101-400C.32 [18_09_07] ■ 01s 101-500C14 [19_09_07]
01s 101_Ref.29 [19_09_07] ■

(a)

N,S_TKP
101_400°C

N,S_TKP
101_500°C

ND_TKP 101

01s 102-400C·26 [18_09_07] ■ 01s 102-500C % [19_09_07] ■
01s 102_Ref.25 [19_09_07] ■

(b)

N,S_TKP102_500°C

ND_TKP102

N,S_TKP102_400°C

Fig. 3. XPS spectra of O 1s peak, in (a) TKP101 powders and (b) TKP102 calcined at 400 and 500 °C.

method used. Interstitial N-doping is favored when the combustion is done under air atmosphere and the substitutional N-doping when the combustion was carried out in the absence of air. Interstitial doping is characterized by the formation of N–O bonds producing mid-gap high-localized states above the top of the valence band around 0.73 eV while substitutional N-doping is located 0.14 eV above this level.
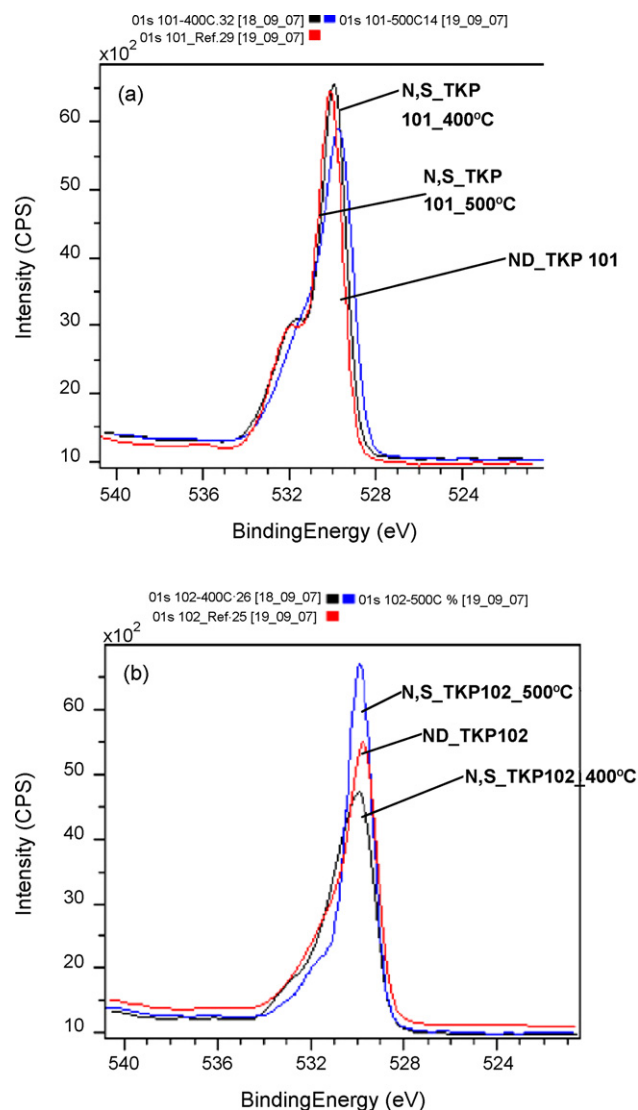
In this work, we found evidence for both types of N-doping. Co-doped TKP101-400 °C, TKP102-400 °C and TKP102-500 °C revealed the presence of N 1s peaks typically assigned to interstitial N-doping. This kind of N-doping seems to be favored since the calcination step was carried out in air atmosphere. However, pure TKP101 revealed two interesting features: absorption at $\lambda < 410$ nm (Fig. 1a) and the presence of N, S and C impurities adsorbed on its surface. TKP101 could then present surface defects such as Ti^{4+} also called oxygen vacancies that favor the adsorption of impurities on TiO_2 surfaces. This would benefit the substitutional N-doping and could also explain the N 1s peak at 395.9 eV on doped TKP101-500 °C. Regarding the S-doping, several reports have suggested anionic (substitution S- by O-doping) and cationic (substitutional S- by Ti-doping). Both types of doping can yield S 3p localized states on the band-gap [55] and these states are responsible of the visible absorption of S-doped TiO_2. We have presented evidence for both types of S-doping in our doped TiO_2.

Table 2 shows the atomic concentration of N and S present on the different powders. Pure TKP101 have N and S species that do not produce visible response on the TiO_2. However, pure and N, S co-doped TKP101 powders showed almost the same atomic

Table 2
Atomic concentration determined by XPS in at.% of N and S present on the surface of non-doped and N, S co-doped powders annealed at 400 and 500 °C

Powder	N 1s (at.%)	S 2s (at.%)
Undoped TKP101	0.84	0.74
Undoped TKP102	0.0	0.0
N, S Tayca TKP101-400 °C	1.00	0.78
N, S Tayca TKP101-500 °C	0.76	0.78
N, S Tayca TKP102-400 °C	0.54	0.71
N, S Tayca TKP102-500 °C	0.80	0.83

concentration of N and S species on the surface. In contrast Tayca TKP102, exhibit an N, S concentration increasing since their N and S atomic concentrations increased only when the doping process was achieved either at 400 and 500 °C.

The absorption in the visible region increases in general with the annealing temperature. We suggest that it is not the quantity but the nature of the N or S doping that determines the optical properties of the doped material since N, S co-doped TKP101-400 °C showed a lower visible absorption than N, S co-doped TKP101-500 °C. This latest material contains substitutional N-doping and cationic substitutional S-doping.

The visible absorption intensity of N, S co-doped TKP102-500 °C was slightly superior to that of N, S co-doped TKP102-400 °C while the N, S species were higher in powders doped at 500 °C. Regarding the nature of the doping species, treated TKP102 materials annealed either at 400 or 500 °C showed interstitial N-doping and ivory coloration. However, it was found that N, S co-doped TKP102-400 °C showed anionic and cationic substitutional S-doping while N, S co-doped TKP102-500 °C showed only cationic substitutional S-doping. This last factor is important in determining the optical properties of the co-doped materials.

In conclusion, we suggest that commercial Tayca TKP101 and TKP102 powders mixed with thiourea and annealed at 400 and 500 °C showed N, S co-doping. N, S co-doping might yield localized mid-band-gap states that under visible light promote electrons to the conduction band (CB).

3.1.3. Specific surface area (BET)

BET experiments were carried out in order to determine the SSA of the materials. Table 3 shows that doped materials present a decreasing in their surface area. In the case of TKP101 powders, the starting material had a SSA around of 300 $m^2 g^{-1}$, and after annealing at 400 and 500 °C their SSA decreased to 249.8 and 207.4 $m^2 g^{-1}$, respectively. N, S co-doped TKP101 calcined at 400 and 500 °C showed an SSA decrease to 286.1 and 220.1 $m^2 g^{-1}$, respectively. Pure TKP102 powder presented an SSA of 110 $m^2 g^{-1}$ and while this TiO_2 calcined at 400 and 500 °C had SSA values of 84.2 and 81.2 $m^2 g^{-1}$, respectively. N, S co-doped TKP102 annealed at 400 and 500 °C showed SSA values of 79.2 and 73.8 $m^2 g^{-1}$.

Table 3
Specific surface area of non-doped and N, S co-doped

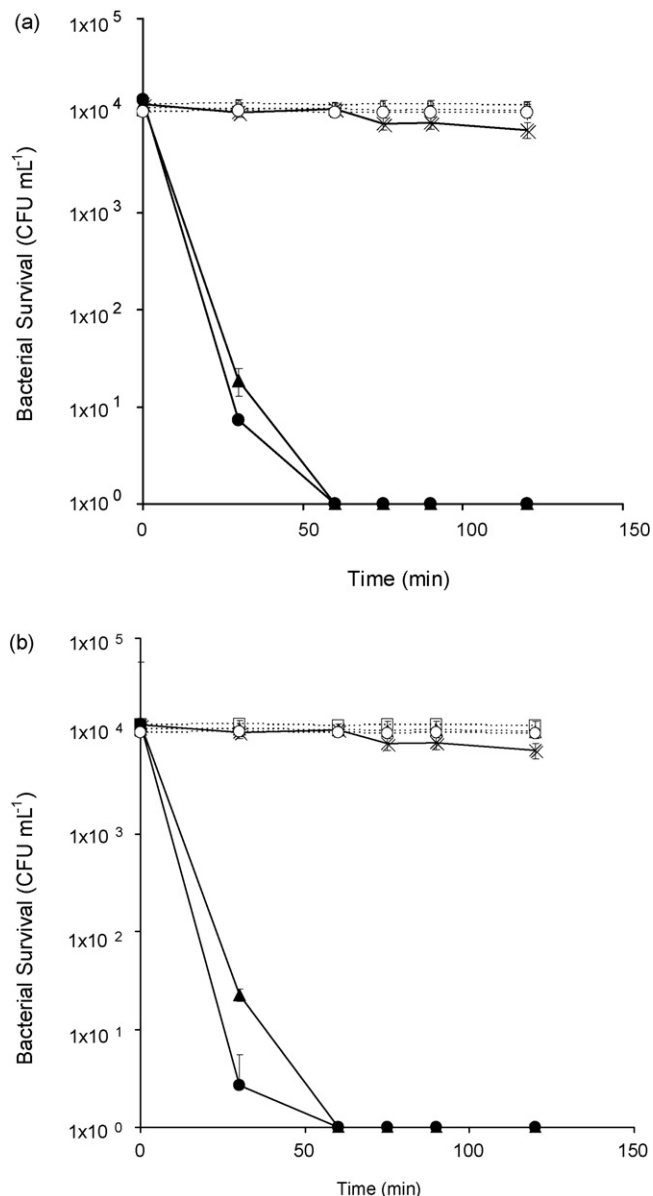| Powder	SSA ($m^2 g^{-1}$)
Undoped TKP101	300
Undoped TKP101-400 °C	249.80
Undoped TKP101-500 °C	207.40
N, S TKP101-400 °C	286.1
N, S TKP101-500 °C	220.1
Undoped TKP102	110
Undoped TKP102-400 °C	84.2
Undoped TKP102-500 °C	81.2
N, S TKP102-400 °C	79.25
N, S TKP102-400 °C	73.88

Fig. 4. Photocatalytic *E. coli* inactivation under UV illumination of (a) TKP101 powders and (b) TKP102 powders. (●) Non-doped powders, (▲) non-doped and N, S co-doped powders annealed at 400 and 500 °C (an average was taken in account since their activities were similar), (△) pure TKP101 + bacteria without light, (□) N, S co-doped TKP101-400 °C + bacteria without light, (○) N, S co-doped TKP101-500 °C + bacteria without light, (*) UV light without catalyst. UV intensity: 38 W m^{-2}, [TiO_2]: 1 g L^{-1} and pH 7.0.

3.2. Photocatalytic activity

3.2.1. Photocatalytic E. coli inactivation on N, S co-doped TiO₂ using black light lamps (UV light)

N, S co-doped TKP101 and TKP102 calcined at 400 and 500 °C showed photocatalytic activity towards *E. coli* inactivation under UV light irradiation (Fig. 4a and b). Dark controls (TiO_2 suspensions + bacteria in the dark) were achieved. These experiments showed that pure and co-doped powders are not toxic for the microorganisms under dark conditions. However, when UV light was present, undoped TKP101 powder showed a better activity than the N, S co-doped TKP101 powder. In the other hand, N, S co-doped TKP102 showed a slightly decrease in their photocatalytic activity in comparison with the pure powder.

However, when non-doped TKP101 and TKP102 powders were annealed at 400 and 500 °C, respectively, their photocatalytic activities were also reduced. Some authors [15,53] suggest that non-metallic doping of TiO_2 powders reduces the photocatalytic activity under UV illumination since the dopant acts as a recombination centers. During the calcinations step, surface dehydroxylation and particle sintering occur with the known detrimental effect on the photocatalytic activity.

XPS analysis of O 1s peak (Fig. 3) showed that the shoulder at BE > 532 eV decreases during the calcination. This shoulder is ascribed to the presence of attached hydroxyl groups or water adsorption on titania surfaces. Hydroxyl groups on TiO_2 surfaces play an important role in photocatalysis. They act as charges trap carriers avoiding charge recombination and producing reactive oxidative species (ROS) responsible for the bacterial inactivation and intervening in the oxidation of chemical substances [60–62].

BET data showed that during the calcinations step, the SSA decreases due to the increase of the TiO_2 particles size. In larger TiO_2 particles, the recombination process has been reported to be favored since electrons and holes cannot easily reach the surface within their lifetimes limiting the formation of surface ROS [63].
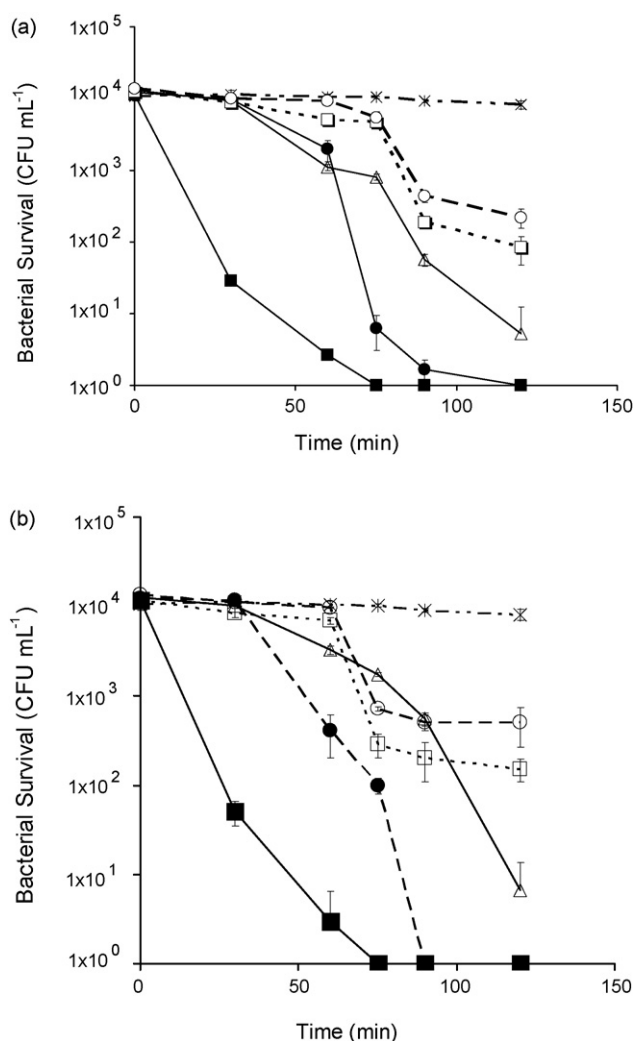

3.2.2. Photocatalytic E. coli inactivation on N, S co-doped TiO_2 using visible light

Fig. 5a and b shows that N, S co-doped TKP powders have the highest photocatalytic activity towards *E. coli* inactivation under visible light illumination compared to pure TKP titania. With pure TKP powders, the total *E. coli* inactivation was not reached within the experimental time. Pure powders presented visible activity probably due that pure TKP101 can absorb radiation below of 410 nm and pure TKP102 below 400 nm. The lamps used emit radiation at these wavelengths allowing to the pure powders produce ROS and inactivate bacterial cells. On the other hand, in this study was used an initial bacterial concentration of 10^4 CFU mL^{-1} and under this experimental conditions, *E. coli* could be more sensible at low ROS concentrations.

N, S co-doped powders calcined at 400 °C present the highest activity under visible light irradiation since the total *E. coli* inactivation was reached in 75 min while in co-doped powders doped at 500 °C 120 min were required.

N, S co-doped TKP101 calcined at 400 °C exhibit the highest *E. coli* inactivation rate, have already been described as having interstitial N-doping and anionic and cationic substitutional S-doping while same material calcined at 500 °C showed only the presence of substitutional N-doping and only cationic S-doping. Calcination of these powders as well as that of N, S co-doped TKP seems to lead to the dehydroxylation and size particle increasing. This suggests that the structure and nature of the doping significantly affects the performance of the photocatalyst during *E. coli* inactivation. This decreases the trapping of the photo-induced charge carriers affecting adversely the production of ROS responsible of the *E. coli* inactivation.

4. Conclusions

Commercial TiO_2 powders Tayca TKP101 and TKP102 showing visible light response were obtained by a relatively simple method, at 400 and 500 °C. Thiourea treated TKP101 powders annealed at 400 °C showed band-gap narrowing around 0.9 eV while material calcined at 500 °C suffered a band-gap narrowing of 0.7 eV. In contrast, doped TKP102 powders annealed either at 400 or 500 °C showed a band-gap narrowing of 0.3 eV. XPS analysis showed that TKP101 and TKP102 present N, S co-doping with different kind of N- and S-doping. N, S co-doped TKP101-400 °C, TKP102-400 and 500 °C present interstitial N-doping. N, S co-doped TKP101-500 °C present substitutional N-doping. Regarding the S-doping, the materials annealed at 400 °C might show anionic and cationic substitutional S-doping while materials annealed at 500 °C only show cationic substitutional S-doping.

The SSA decreased in annealed non-doped and doped materials as expected. N, S co-doped materials showed photocatalytic activity under UV illumination towards *E. coli* inactivation. Co-doped powders showed a highest photocatalytic activity towards *E. coli* inactivation compared to the pure materials under visible light (400–500 nm) irradiation. However, when the calcination temperature was raised to 500 °C, co-doped powders showed a diminution of their photocatalytic activities.

We suggest that the photocatalytic activity of commercial N, S co-doped TKP powders depend of the nature of the doping (either substitutional or interstitial N-doping and cationic or anionic S-doping), the hydroxylation degree and the size particle.

Fig. 5. Photocatalytic *E. coli* inactivation under blue light illumination of (a) TKP101 powders and (b) TKP102 powders. (△) Non-doped powders, (■) N, S co-doped powders annealed at 400 °C, (●) N, S co-doped powders annealed at 500 °C, (*) blue light without catalyst, (□) pure powder annealed at 400 °C, (○) pure powder annealed at 500 °C. Total light intensity: 60 W m^{-2} and UV intensity: 0.1 W m^{-2}, [TiO_2]: 1 g L^{-1} and pH 7.0.

References

[1] S.D. Richardson, T.A. Ternes, Anal. Chem. 77 (2005) 3807–3838.
[2] A. Mills, R. Davies, D. Worsley, Chem. Soc. Rev. 22 (1993) 417–425.
[3] A. Fujishima, T.N. Rao, D.A. Tryk, J. Photochem. Photobiol. C 1 (2000) 1–21.
[4] M.R. Hoffmann, S.T. Martin, W. Choi, D.W. Bahnemann, Chem. Rev. 95 (1995) 69–169.
[5] J.M. Herrmann, Catal. Today 53 (1999) 115–129.
[6] A.L. Linsebigler, G. Lu, J.T. Yates, Chem. Rev. 95 (1995) 735–758.
[7] D.M. Blake, P.Ch. Maness, Z. Huang, E.J. Wolfrum, J. Huang, W.A. Jacoby, Sep. Purif. Methods 28 (1999) 1–50.
[8] A.G. Rincon, C. Pulgarin, Appl. Catal. B 49 (2004) 99–112.
[9] V. Nadtochenko, A.G. Rincon, S.E. Stanca, J. Kiwi, J. Photochem. Photobiol. A 169 (2005) 131–137.
[10] J. Wist, J. Sanabria, C. Dierolf, W. Torres, C. Pulgarin, J. Photochem Photobiol. A 147 (2002) 241–246.
[11] D. Gumy, C. Morais, P. Bowen, C. Pulgarin, S. Giraldo, R. Hadju, J. Kiwi, Appl. Catal. B: Environ. 63 (2006) 76–84.
[12] L. Lucarelli, V. Nadtochenko, J. Kiwi, Langmuir 16 (2000) 1102–1108.
[13] T. Wu, G. Lin, J. Zhao, H. Hidaka, N. Serpone, J. Phys. Chem. B 103 (1999) 4862–4867.
[14] J. Hodak, C. Quinteros, M.I. Litter, E.S. Roman, J. Chem. Soc. Faraday Trans. 92 (1996) 5081–5088.
[15] M. Anpo, S. Dohshi, M. Kitano, Y. Hu, M. Takeuchi, M. Matsuoka, Annu. Rev. Mater. Res. 35 (2005) 1–27.
[16] M. Kitano, M. Matsuoka, M. Ueshima, Anpo Appl. Catal. A 325 (2007) 1–14.
[17] H. Yamashita, M. Harada, J. Misaka, M. Takeuchi, M. Ikeue, M. Anpo, J. Photochem. Photobiol. A 148 (2002) 257–261.
[18] J.C.S. Wu, C.H. Chen, J. Photochem. Photobiol A 163 (2004) 509–515.
[19] T. Ihara, M. Miyoshi, M. Ando, S. Sugihara, Y. Iriyama, J. Mater. Sci. 36 (2001) 4201–4207.
[20] T. Ihara, M. Miyoshi, Y. Iriyama, O. Matsumoto, S. Sugihara, Appl. Catal. B: Environ. 42 (2003) 403–409.
[21] J. Chen, L.B. Lin, F.Q. Jing, J. Phys. Chem. Solid. 62 (2001) 1257–1262.
[22] S. Sato, R. Nakamura, S. Abe, Appl. Catal. A 284 (2005) 131–137.
[23] Y. Cong, J. Zhang, F. Chen, M. Anpo, J. Phys. Chem. C 111 (2007) 6976–6982.
[24] T. Ohno, M. Akiyoshi, T. Umebayashi, K. Asai, T. Mitsui, M. Matsamura, Appl. Catal. A 265 (2004) 115–121.
[25] R. Silveyra, L. De la Torre Sáenz, W. Antúnez-Flores, V. Collins-Martínez, A. Aguilar-Elguézabal, Catal. Today 107/108 (2005) 602–605.
[26] J.M. Gole, J.D. Stout, C. Burda, Y. Lou, X. Chen, J. Phys. Chem. B 108 (2004) 1230–1240.
[27] R. Bacsa, J. Kiwi, T. Ohno, P. Albers, V. Nadtochenko, J. Phys. Chem. B 109 (2005) 5994–6003.
[28] T. Ihara, M. Miyoshi, Y. Iriyama, O. Matsumoto, S. Sugihara, Appl. Catal. B 42 (2003) 403–409.
[29] R. Asahi, T. Morikawa, T. Ohwaki, K. Aoki, Y. Taga, Science 293 (2001) 269–271.
[30] S. Livraghi, A.M. Votta, M.C. Paganini, E. Giamello, Chem. Commun. 4 (2005) 498–500.
[31] C. Di Valentin, G. Pacchioni, A. Selloni, S. Livraghi, E. Giamello, J. Phys. Chem. B 109 (2005) 11414–11419.
[32] S. Livraghi, M.C. Paganini, E. Giamello, A. Selloni, C. Di Valentin, G. Pacchioni, J. Am. Chem. Soc. 128 (2006) 15666–15671.
[33] C. Di Valentin, G. Pacchioni, A. Selloni, Chem. Mater. 17 (2005) 6656–6665.
[34] T. Umebayashi, T. Yamaki, H. Itoh, K. Asai, Appl. Phys. Lett. 81 (2002) 454–456.
[35] S. Sakthivel, H. Kisch, Chem. Phys. Chem. 4 (2003) 487–490.
[36] T. Ohno, T. Mitsui, M. Matsumura, Chem. Lett. 32 (2003) 364–365.
[37] M.S. Wong, W.Ch. Chu, D.S. Sun, H.S. Huang, J.H. Chen, P.J. Tsai, N.T. Lin, M.S. Yu, S.F. Hsu, S.L. Wang, H.H. Chang, Appl. Environ. Microbiol. 72 (2006) 6111–6116.
[38] Y. Liu, J. Li, X. Qiu, C. Burda, J. Photochem. Photobiol A 190 (2007) 94–100.
[39] J.C. Yu, W. Ho, J. Yu, H. Yip, P.K. Wong, J. Zhao, Environ. Sci. Technol. 39 (2005) 1175–1179.
[40] D. Mitoraj, A. Janczyk, M. Strus, H. Kisch, G. Stochel, P.B. Heczko, W. Macyk, Photochem. Photobiol. Sci. 6 (2007) 642–648.
[41] S. Yin, K. Ihara, Y. Aita, M. Komatsu, T. Sato, J. Photochem. Photobiol. A 179 (2006) 105–114.
[42] J. Yu, M. Zhou, B. Cheng, X. Zhao, J. Mol. Catal. A 246 (2006) 176–184.
[43] P. Kubelka, F. Munk, Zei. Tech. Phys. 12 (1931) 593–601.
[44] A. Nambu, J. Graciani, J.A. Rodriguez, Q. Wu, E. Fujita, J.J. Fernandez-Sanz, Chem. Phys. 125 (2006) 094706-1–094706-8.
[45] H. Irie, S. Washizuka, N. Yoshino, K. Hashimoto, Chem. Commun. 11 (2003) 1298–1299.
[46] O. Diwald, T.L. Thompson, E.G. Goralski, S.D. Walck, J.T. Yates, J. Phys. Chem. B 108 (2004) 52–57.
[47] J.A. Rodriguez, T. Jirsak, G. Liu, J. Hrbek, J. Dvorak, A. Maiti, J. Am. Chem. Soc. 123 (2001) 9597–9605.
[48] U. Diebold, Surf. Sci. Rep. 48 (2003) 53–229.
[49] N.C. Saha, H.G. Tompkins, J. Appl. Phys. 72 (1992) 3072–3079.
[50] X. Chen, Y. Lou, A.C. Samia, C. Burda, J.L. Gole, Adv. Funct. Mater. 15 (2005) 41–49.
[51] O. Diwald, T.L. Thompson, E.G. Goralski, S.D. Walck, J.T. Yates, J. Phys. Chem. B 108 (2004) 6004–6008.
[52] M. Sathish, B. Viswanathan, R.P. Viswanath, C.S. Gopinath, Chem. Mater. 17 (2005) 6349–6353.
[53] H. Sun, Y. Bai, Y. Cheng, W. Jin, N. Xu, Ind. Eng. Chem. Res. 45 (2006) 4971–4976.
[54] W. Ho, J.C. Yu, S. Lee, J. Solid State Chem. 179 (2006) 1171–1176.
[55] T. Umebayashi, T. Yamaki, A. Yamamoto, A. Miyashita, S. Tanaka, T. Sumita, K. Asai, J. Appl. Phys. 93 (2003) 5156–5160.
[56] E.L.D. Hebenstreit, W. Hebenstreit, U. Diebold, Surf. Sci. 470 (2001) 347–360.
[57] G. Colón, H. Hidalgo, G. Munuera, I. Ferino, M.G. Cutrufello, J.A. Navío, Appl. Catal. B 63 (2006) 45–59.
[58] E. Gyorgy, A. Perez del Pino, P. Serra, J.L. Morenza, Surf. Coat. Technol. 173 (2003) 265–270.
[59] X. Chen, C. Burda, J. Phys. Chem. B 108 (2004) 15446–15449.
[60] N.R.C. Fernandez Machado, V.S. Santana, Catal. Today 107/108 (2005) 595–601.
[61] K.S. Finnie, D.J. Cassidy, J.R. Bartlett, J.L. Woolfrey, Langmuir 17 (2001) 816–820.
[62] S.H. Szczepankiewicz, A.J. Colussi, M.R. Hoffmann, J. Phys. Chem. B 104 (2000) 9842–9850.
[63] C.B. Almquist, P. Biswas, J. Catal. 212 (2002) 145–156.